

Thermal activation in bistable systems under external periodic forces

P. Jung

Institut für Mathematik, Universität Augsburg, Federal Republic of Germany

Received February 6, 1989; revised version May 16, 1989

Considered is the motion of a Brownian particle in a bistable potential exposed to an external periodic field. Our analysis is based on a systematic Fokker-Planck description of the non-stationary stochastic process. Besides general characteristics, such as the non-mixing property, we present full numerical solutions for probability distributions and the modulation induced rate enhancement. Moreover, approximation schemes for small and large frequencies are considered and their results are compared to the numerical data.

1. Introduction

Stochastic activation processes in metastable systems are of importance in a number of fields in physics. In his pioneering work, Kramers [1] studied the escape of a Brownian particle over a barrier. Kramers succeeded in solving the corresponding Fokker-Planck equation (FPE) for the escape rate in the case of large and small damping in the low-temperature limit. In the following years his results have been improved and extended to more general situations [2], including for instance memory effects.

In many physical situations, there are additional periodic fields which assist the system in passing a potential barrier. In the case of an underdamped Van der Pol oscillator (linear force-field, nonlinear friction), such a problem has been discussed in the context of noise induced phase slips in [3]. The linearly damped duffing oscillator (non-linear force field) driven by white noise and periodic forces has been studied by using numerical simulations in [4]; for the inverted double well potential similar calculations have been performed in [5]. The main focus in [4] and [5] is on the power spectrum of the stochastic output signal, where the low-frequency part is related to the escape rates out of a region of attraction. The problem of the escape of an underdamped Brownian particle out of a metastable state with periodic forcing has been studied in terms of a low friction expansion of the

Kramers equation by Carmely and Nitzan in [6]. They, however, had to introduce a finite coherence time in their external field, in order to avoid resonance between the external field and higher harmonics of the well oscillations. Also in [7], the effect of an external field with finite coherence time on a Brownian particle is discussed. A semiclassical study of the escape in a metastable potential is done by Larkin and Ovchinnikov [8]; the transition from quantum- to classical dissipation is discussed by Chow and Ambegaokar [9] in the weak damping limit.

In this paper I consider the *overdamped* dynamics of a Brownian particle in a bistable potential exposed to an external periodic coherent field. Though there is no resonant interaction between the field and the internal degrees of freedom and thus no resonantly activated barrier crossing, this problem is of practical interest for instance in connection with Josephson junctions [10] and in the context of “stochastic resonance [11]”. The stochastic resonance effect is the resonant increase of the signal/noise ratio of the output-signal in a bistable system modulated by periodic forces as a function of the noise strength. Moreover, this problem is of general theoretical interest with respect to the interplay between nonlinearity, noise and the external field. In an earlier letter [12] we have considered the asymptotic probability distributions for large times, the dynamical susceptibilities and the correlation functions. This paper is mainly

devoted to the escape process out of a region of attraction in an one dimensional bistable potential. This paper is organized as follows:

In Sect. 2 the model and the basic concepts used in this paper are introduced. The equivalence of an one-dimensional description in terms of quasi-spectral properties and a two-dimensional description in terms of eigenvalues and eigenfunctions is shown. In Sect. 3, full numerical solutions for the asymptotic distribution function and the transition rates, obtained by using a matrix continued fraction technique [13], are presented. Analytical approximations for the probability distributions and the transition rate at small and large field frequencies are discussed in Sect. 4. Finally in Sect. 5 the influence of an additional phase diffusion term on the spectral, dynamical and static properties is discussed.

2. Basic concepts

2.1. General theory

Brownian motion is usually described in terms of Langevin equations. These equations are the Newtonian equations of motion supplemented by a stochastic force $\zeta(t)$ (noise), characterized by its statistical properties. The noise simulates the interaction of the Brownian particle with its environment being in thermodynamic equilibrium with the Brownian particle itself. Throughout this paper we assume Gaussian, delta correlated (white) noise $\zeta(t)$ with zero mean. The external periodic field is modeled by a sineshaped modulation of the Langevin equation. For the underlying potential we choose the archetype bistable potential

$$V(x) = -\frac{1}{2} ax^2 + \frac{1}{4} bx^4. \quad (2.1)$$

having minima at $x_{1,2} = \pm\sqrt{a/b}$, and a saddle point at $x=0$. The barrier height is $\Delta V = a^2/4b$. The Langevin equation governing the dynamics of our model reads

$$\begin{aligned} \dot{x} &= ax - bx^3 + A \sin(\omega_0 t + \phi) + \zeta(t) \\ \langle \xi(t) \xi(t') \rangle &= 2D\delta(t-t') \\ \langle \xi(t) \rangle &= 0, \end{aligned} \quad (2.2)$$

where D is the noise strength, A the modulation strength and ω_0 the modulation frequency. In (2.2) an additional random phase ϕ has been introduced to take into account the generally unknown initial phase of the external field. As a first step we introduce dimensionless variables and parameters $\bar{x} = \sqrt{b/a}x$, $\bar{t} = at$, $\bar{A} = A\sqrt{b/a^3}$, $\bar{\omega}_0 = \omega_0/a$ and $\bar{D} = Db/a^2$.

Since this scaling is used throughout this paper we omit the bars from now on. In scaled variables, the Langevin equation (2.2) thus reads

$$\dot{x} = x - x^3 + A \sin(\omega_0 t + \phi) + \zeta(t), \quad (2.3)$$

where the statistical properties of the noise $\zeta(t)$ are the same as in (2.2). Since (2.3) describes a nonstationary Markovian process the statistically equivalent one dimensional Fokker-Planck equation (FPE) reads

$$\begin{aligned} \frac{\partial P(x, t)}{\partial t} &= -\frac{\partial}{\partial x} (x - x^3 + A \sin(\omega_0 t + \phi)) P(x, t) \\ &\quad + D \frac{\partial^2}{\partial x^2} P(x, t) \\ &= \left(\mathcal{L}_0 - A \frac{\partial}{\partial x} \sin(\omega_0 t + \phi) \right) P(x, t) \end{aligned} \quad (2.4)$$

where the drift coefficient contains a time periodic part and where

$$\mathcal{L}_0 = -\frac{\partial}{\partial x} (x - x^3) + D \frac{\partial^2}{\partial x^2}. \quad (2.5)$$

The discrete time translation symmetry of the drift coefficient with the period $T = 2\pi/\omega_0$ allows a Floquet-ansatz for the solution of (2.4), i.e. we seek for solutions of the form [12, 13]

$$\begin{aligned} P^\mu(x, t) &= \exp(-\mu t) \rho_\mu(x, t) \\ \rho_\mu(x, t) &= \rho_\mu(x, t + T). \end{aligned} \quad (2.6)$$

We term the quantities μ quasi-eigenvalues and the complex functions $\rho_\mu(x, t)$ quasi-eigenfunctions. The general solution of (2.4) may be expressed as a superposition of $\{P^\mu(x, t)\}$, which we assume to be complete. This procedure is in analogy to the quasi-energy concept in quantum mechanical systems [14] with a periodic driving. Expanding the periodic function $\rho_\mu(x, t)$ into a Fourier series

$$\rho_\mu(x, t) = \sum_{n=-\infty}^{\infty} p_n^\mu(x) \exp(in(\omega_0 t + \phi)) \quad (2.7)$$

and inserting (2.6) and (2.7) into the FPE (2.4) we find the infinite hierarchy of partial differential equations for the complex functions $p_n^\mu(x)$

$$\begin{aligned} (\mathcal{L}_0 - (in\omega_0 - \mu) 1) p_n^\mu(x) - \frac{1}{2} iA \frac{\partial}{\partial x} (p_{n+1}^\mu(x) \\ - p_{n-1}^\mu(x)) = 0. \end{aligned} \quad (2.8)$$

In order to obtain (2.8) one has to use the orthogonality of the trigonometric functions.

An alternative concept for treating the nonstationary Markovian process (2.3) is to avoid the time dependent drift coefficient by extending the Langevin equation (2.3) to the two dimensional system

$$\begin{aligned}\dot{x} &= x - x^3 + A \sin(\theta) + \xi(t) \\ \dot{\theta} &= \omega_0,\end{aligned}\quad (2.9)$$

being a stationary Markovian pair process in x and θ . The additional phase variable θ is a random variable due to its random initial condition $\theta(0) = \phi$. The corresponding two dimensional time homogeneous Fokker-Planck equation reads

$$\begin{aligned}\frac{\partial W(x, \theta, t)}{\partial t} &= \left(\mathcal{L}_0 - A \sin(\theta) \frac{\partial}{\partial x} - \omega_0 \frac{\partial}{\partial \theta} \right) W(x, \theta, t) \\ &= \mathcal{L}_{\mathcal{F}\phi} W(x, \theta, t).\end{aligned}\quad (2.10)$$

In order to solve (2.10) we have to specify boundary conditions

$$\begin{aligned}W(x \rightarrow \pm \infty, \theta, t) &= 0 \\ W(x, \theta, t) &= W(x, \theta + 2\pi, t).\end{aligned}\quad (2.11)$$

The natural boundary conditions in x are appropriate for a confining potential (such as the quartic double well potential) and the periodic boundary conditions in θ are chosen, since the random phase θ is observable only modulo 2π . Expanding $W(x, \theta, t)$ into a Fourier series with respect to θ

$$W(x, \theta, t) = \sum_{n=-\infty}^{\infty} c_n(x, t) \exp(in\theta), \quad (2.12)$$

and inserting this expansion into (2.10) we obtain after some algebraic manipulations the infinite hierarchy of partial differential equations for the complex-valued functions $c_n(x)$, i.e.

$$\begin{aligned}\dot{c}_n &= (\mathcal{L}_0 - in\omega_0) c_n(x, t) - iA \frac{1}{2} \frac{\partial}{\partial x} \\ &\quad (c_{n+1}(x, t) - c_{n-1}(x, t)).\end{aligned}\quad (2.13)$$

Since the Fokker-Planck operator $\mathcal{L}_{\mathcal{F}\phi}$ in (2.10) is time independent it has well defined eigenvalues and eigenfunctions, i.e. (2.10) has solutions of the form $p(x, \theta) \exp(-\lambda t)$. For the coefficients the corresponding ansatz

$$c_n(x, t) = k_n(x) \exp(-\lambda t) \quad (2.14)$$

leads to the linear infinite system of differential equations for the complex coefficients $k_n(x)$

$$\begin{aligned}0 &= (\mathcal{L}_0 - (in\omega_0 - \lambda) 1) k_n(x) - iA \frac{1}{2} \frac{\partial}{\partial x} \\ &\quad \cdot (k_{n+1}(x) - k_{n-1}(x)).\end{aligned}\quad (2.15)$$

Since (2.14) and (2.8) are identical we can make the important conclusion [12]: *The eigenvalues of the two dimensional FPE (2.10) are identical to the quasi-eigenvalues of the one dimensional FPE (2.4) with time periodic drift coefficients.* This conclusion allows to apply the well known spectral theorems for time independent Fokker-Planck operators [15] to our time dependent problem by studying the extended two dimensional FPE. Although two dimensional Fokker-Planck equations seem to be well understood for a number of particular systems [13], our FPE (2.10) requires much care concerning initial preparation effects and ergodic properties. The origin of this complications is a branch of purely imaginary eigenvalues of the Fokker-Planck operator in (2.10) which does not occur in standard Brownian motion problems, or Fokker-Planck equations for the laser [13]. This branch can be derived from the hermitian adjoint eigenvalue equation corresponding to (2.10), i.e.

$$\begin{aligned}\mathcal{L}_{\mathcal{F}\phi}^\dagger \varphi_n(x, \theta) &= -\lambda_n \varphi_n(x, \theta) \\ \mathcal{L}_{\mathcal{F}\phi}^\dagger &= \mathcal{L}_0^\dagger + A \sin \theta \frac{\partial}{\partial x} + \omega_0 \frac{\partial}{\partial \theta}.\end{aligned}\quad (2.16)$$

The ansatz for x -independent left-eigenfunctions

$$\varphi_n(x, \theta) = \varphi_{0n}(\theta) \quad (2.17)$$

leads to the ordinary eigenvalue problem

$$\begin{aligned}\omega_0 \frac{\partial}{\partial \theta} \varphi_{0n}(\theta) &= -\lambda_{0n} \varphi_{0n} \\ \varphi_{0n}(\theta) &= \varphi_{0n}(\theta + 2\pi),\end{aligned}\quad (2.18)$$

with the solution

$$\begin{aligned}\varphi_{0n}(\theta) &= \exp(-in\theta) \\ \lambda_{0n} &= in\omega_0 \quad n = \pm 1, \pm 2, \dots\end{aligned}\quad (2.19)$$

A consequence of the existence of the branch of purely imaginary eigenvalues is the non-mixing property of the Fokker-Planck equation (2.10) as shown in the following. The dynamics of the x -integrated probability density

$$\rho(\theta, t) = \int W(x, \theta, t) dx \quad (2.20)$$

is given by the equation of motion

$$\frac{\partial \rho(\theta, t)}{\partial t} = -\omega_0 \frac{\partial}{\partial \theta} \rho(\theta, t) \quad (2.21)$$

which is obtained by formal integration of the FPE (2.10). The solution of (2.21) with the initial condition $\rho(\theta, 0) = h(\theta)$ reads

$$\rho(\theta, t) = h(\theta - \omega_0 t). \quad (2.22)$$

The probability density $\rho(\theta, t)$ does not approach a stationary distribution, unless one already starts with a uniform distribution in θ (implying uniformly distributed initial phases ϕ), i.e.

$$\rho(\theta, t=0) = \frac{1}{2\pi}. \quad (2.23)$$

This behavior is a direct consequence of the purely imaginary eigenvalues, since the positive real part of the eigenvalues of a Fokker-Planck equation is responsible for the relaxation towards a steady state. The solution (2.22) of (2.21) describes a dispersion-free shift (modulo 2π) of the initial distribution with velocity ω_0 . Hence, the solutions with respect to two non-overlapping initial distributions $h(\theta)$ on $[0, 2\pi]$ do not mix in course of time, i.e. they do not overlap on $[0, 2\pi]$. The FPE (2.10) is thus *non-mixing on a functional subspace* spanned up by the eigenfunctions corresponding to the purely imaginary eigenvalues [12].

2.2. Asymptotic probability distributions for large times

Since the one dimensional Markovian process (2.2), described by the FPE (2.4) is with time-periodic drift component, an initial probability $P(x, 0)$ does not decay to a stationary distribution. Instead, for large times $P(x, t)$ approaches a periodic asymptotic probability distribution $P_{as}^\phi(x, t)$, which is not unique, but depends on the initial phase ϕ . For a uniformly distributed initial phase [12] the *two dimensional* probability $W(x, \theta, t)$ converges to a stationary distribution function $W_{st}(x, \theta)$ which is determined by (2.10) with $\partial W / \partial t = 0$, i.e.

$$0 = \left(\mathcal{L}_0 - A \sin \theta \frac{\partial}{\partial x} - \omega_0 \frac{\partial}{\partial \theta} \right) W_{st}(x, \theta). \quad (2.24)$$

Performing the variable transform $\theta \rightarrow s$, with

$$\begin{aligned} \theta &= \omega_0 s + \phi \\ \tilde{W}^\phi(x, s) &= 2\pi W_{st}(x, \omega_0 s + \phi). \end{aligned} \quad (2.25)$$

we find

$$\frac{\partial \tilde{W}^\phi(x, s)}{\partial s} = \left(\mathcal{L}_0 - A \sin(\omega_0 s + \phi) \frac{\partial}{\partial x} \right) \tilde{W}^\phi(x, s). \quad (2.26)$$

To be consistent with the periodic boundary conditions in (2.11) we require periodicity in s , i.e.

$$\tilde{W}^\phi(x, s) = \tilde{W}^\phi\left(x, s + \frac{2\pi}{\omega_0}\right). \quad (2.27)$$

Equation (2.26) has the same form as the FPE (2.4) of the original one dimensional time dependent problem. The variable s in (2.26) plays the role of the time. Since (2.26) requires periodic boundary conditions (2.27) in s , we conclude that the asymptotic solution of the FPE (2.4) $P_{as}^\phi(x, t)$, which is periodic in t , is identical with $\tilde{W}^\phi(x, t)$, i.e.

$$P_{as}^\phi(x, t) = \tilde{W}^\phi(x, t) = 2\pi W_{st}(x, \omega_0 t + \phi). \quad (2.28)$$

In other words, the stationary distribution of the two dimensional FPE (2.10) is, apart from a normalization constant identical, with the asymptotic probability of the one dimensional FPE (2.4), with θ being interpreted as a scaled time.

The *phase averaged asymptotic distribution*, defined by

$$\bar{P}_{as}(x) = \frac{1}{2\pi} \int_0^{2\pi} P_{as}^\phi(x, t) d\phi, \quad (2.29)$$

is related to the θ -integrated two dimensional stationary distribution, $W_{st}(x, \theta)$ by

$$\begin{aligned} \bar{P}_{as}(x) &= \int_0^{2\pi} W_{st}(x, \omega_0 t + \phi) d\phi \\ &= \int_0^{2\pi} W_{st}(x, \theta) d\theta \equiv \hat{W}_{st}(x). \end{aligned} \quad (2.30)$$

In deriving (2.30) we have used (2.28) and the periodicity of $W_{st}(x, \theta)$ in θ . In contrast to the asymptotic probability $P_{as}^\phi(x, t)$ with given phase ϕ , the *phase averaged distribution* $\bar{P}_{as}(x)$ is not time dependent. Note, that this property holds only true for uniformly distributed initial phases ϕ .

At this point I want to emphasize that phase averaging does not restore the strong-mixing behavior (i.e. $\langle x(t)x(0) \rangle \rightarrow \langle x \rangle^2$ for $t \rightarrow \infty$) of correlation functions, even not if we initially start with uniformly distributed phases ϕ [16]. Correlation functions (more generally quantities depending on more than one time argument) exhibit after phase averaging ever present undamped periodic oscillations [12]. This problem has

recently lead to some confusion in the context of stochastic resonance, since the power – spectra of such processes contain δ -spikes [11 b, 12, 17].

2.3. Transition rates

Since our potential is bistable the particle can escape from one region of attraction to the other. Without the time-periodic external field the transition rate between the two regions of attraction is given for small noise strength D by one half of the smallest non-vanishing eigenvalue of the Fokker-Planck operator \mathcal{L}_0 [13, 15]. This is a consequence of the fact that there is only one eigenvalue which converges exponentially to zero for increasing Arrhenius factor $\Delta V/D$. The other eigenvalues are well separated from this smallest non-vanishing eigenvalue. Thus, this smallest non-vanishing eigenvalue determines the dynamics of a population for large times, and therefore the rate of escape. Within a saddle point approach this eigenvalue is twice the Kramers rate and reads

$$\lambda_0 = \frac{\sqrt{2}}{\pi} \exp\left(-\frac{\Delta V}{D}\right) \quad (2.31)$$

with the barrier height $\Delta V = 0.25$.

With the time-periodic external field the two dimensional Fokker-Planck operator in (2.10) cannot be transformed to a Hermitian operator. Thus the eigenvalues may generally be complex. In this case the smallest non-vanishing real part can be identified with the transition rate. At first glance this identification seems to be questionable for extremely small modulation frequencies ($\omega_0 \ll \lambda_0$) since in this limit the largest time scale is not the escape time, but rather the periodic modulation of the potential. Based on numerical calculations presented below it turns out (i) that there are no other complex eigenvalues than those of the purely imaginary branch (vanishing real part) and (ii) that the real eigenvalues *increase* with decreasing frequency ω_0 . Thus, the smallest non-vanishing real eigenvalue is not connected dynamically to the purely periodic modulation of the potential but rather represents the enhanced thermal escape rate, even for vanishing small modulation frequencies.

3. Numerical solution with matrix continued fractions

3.1. General technique

In order to calculate the eigenvalues, eigenfunctions and the stationary distribution, we have to solve (2.15) numerically. In a first step we expand the coefficients

$k_n(x)$ into the complete orthogonal set of Hermite functions $\{\psi_n(x)\}$

$$k_n(x) = \rho_0(x) \sum_{m=0}^{\infty} c_n^m \psi_m(x), \quad (3.1 a)$$

$$\psi_m(x) = \sqrt{\frac{\alpha}{n! 2^n \sqrt{\pi}}} H_n(\alpha x) \exp\left(-\frac{1}{2} \alpha^2 x^2\right) \quad (3.1 b)$$

where $H_n(x)$ are the Hermite polynomials and the constant α is a arbitrary scaling parameter. The function $\rho_0(x)$ is a shape function, used to improve on the convergence of the matrix continued fraction technique. Inserting (3.1 a) into (2.15) and using the orthogonality and recursion properties of Hermite-polynomials we finally obtain

$$\sum_{m'=0}^{\infty} Q_{m,m'}(n) c_n^{m'} + Q_{m,m'}^+ c_{n+1}^{m'} + Q_{m,m'}^- c_{n-1}^{m'} = 0, \quad (3.2)$$

with the complex-valued matrices

$$\begin{aligned} Q_{m,m'}(n) &= L_0^{m,m'} - i n \omega_0 \delta_{m,m'} + \lambda \delta_{m,m'} \\ Q_{m,m'}^+ &= -\frac{1}{2} i A B_{m,m'} = -Q_{m,m'}^- \end{aligned} \quad (3.3)$$

The matrices $L_0^{m,m'}$ and $B_{m,m'}$ are given explicitly in Appendix A. Introducing the column matrices

$$\underline{c}_n = (c_n^0, c_n^1, c_n^2, c_n^3 \dots)^T \quad (3.4)$$

we finally obtain the tridiagonal vector recurrence relation

$$\mathbf{Q}_n(\lambda) \underline{c}_n + \mathbf{Q}^+ \underline{c}_{n+1} + \mathbf{Q}^- \underline{c}_{n-1} = 0 \quad (3.5)$$

which forms the basis of our numerical investigations. Such vector recurrence relations can be solved (downward) in terms of matrix continued fractions [13]. Inserting the ansatz

$$\mathbf{S}_n \underline{c}_n = \underline{c}_{n+1} \quad (3.6)$$

into (3.5) one readily finds the two-point recursion for \mathbf{S}_n

$$\mathbf{S}_{n-1}(\lambda) = -[\mathbf{Q}_n(\lambda) + \mathbf{Q}^+ \mathbf{S}_n(\lambda)]^{-1} \mathbf{Q}^-, \quad (3.7)$$

which can be solved iteratively for \mathbf{S}_0 , yielding

$$\mathbf{S}_0(\lambda) = \frac{1}{\mathbf{Q}_1(\lambda) - \mathbf{Q}^+ \frac{1}{\mathbf{Q}_2(\lambda) - \mathbf{Q}^+ \frac{1}{\mathbf{Q}_3(\lambda) \dots} \mathbf{Q}^-} \mathbf{Q}^-} \quad (3.8)$$

The fractions denote matrix inversions. Inserting (3.6) into (3.5) for $n=0$ yields the determinantal condition for the eigenvalues λ

$$\det[\mathbf{Q}_0(\lambda) + \mathbf{Q}^+ \mathbf{S}_0(\lambda) + (\mathbf{Q}^+ \mathbf{S}_0(\lambda^*))^*] = 0. \quad (3.9)$$

In deriving (3.9) we have used the identity $\underline{c}_m(\lambda) = \underline{c}_{-m}^*(\lambda^*)$. The complex valued eigenvalues are obtained from the complex-valued determinantal condition (3.9) by using a two dimensional regula falsi. Note, however, that the purely imaginary eigenvalues $\lambda_{0m} = \text{im } \omega_0$ cannot be found with (3.8) and (3.9). The reason is that the matrix inversion in (3.7) is not possible for $n=m$, since the occurring matrix $\mathbf{Q}_m(\lambda = \text{im } \omega_0) + \mathbf{Q}^+ \mathbf{S}_m(\lambda = \text{im } \omega_0)$ has a vanishing determinant [18]. The same problem occurs in the calculation of the stationary distribution $W_{st}(x, \theta)$ ($\lambda=0$) for $\omega_0 = 0$. For *real* eigenvalues λ_r , the coefficients \underline{c}_0 are real ($\underline{c}_n(\lambda_r) = \underline{c}_{-n}^*(\lambda_r)$) and (3.9) is simplified to

$$\det[\mathbf{Q}_0(\lambda_r) + 2 \text{Re}(\mathbf{Q}^+ \mathbf{S}_0(\lambda_r))] = 0. \quad (3.10)$$

The MCF technique is also useful for finding approximations for the reduced one dimensional probability distributions. As shown in appendix B it is possible to derive an exact master-like equation for the phase averaged probability distribution.

Finally I want to remark, that one can reduce the numerical computation times by making use of the particular symmetry of the eigenfunctions, valid for a symmetric potential $V(x) = V(-x)$

$$\begin{aligned} \Phi^+(x, \theta) &= \Phi^+(-x, \theta + \pi) \\ \Phi^-(x, \theta) &= -\Phi^-(-x, \theta + \pi). \end{aligned} \quad (3.11)$$

The splitting into two symmetry classes follows from the fact that the symmetry operator $\hat{\sigma}: (x \rightarrow -x, \theta \rightarrow \theta + \pi)$ commutes with the Fokker-Planck operator in (2.10). In the expansion of $\Phi^\pm(x, \theta)$ into trigonometric functions with respect to θ and Hermite functions $\psi_n(x)$ with respect to x , only those terms $\psi_n(x) \exp(\text{im } \theta)$ with the correct symmetry have to be taken into account. This reduces the computation times by approximately a factor of 8. However, to keep this technical section as general as possible (allowing also asymmetric potentials) we don't use this particular symmetry.

3.2. Asymptotic probability density for large times

As shown in Sect. 2, the asymptotic probability density is given by the stationary distribution of the two dimensional Fokker-Planck equation (2.10) being the eigenfunction corresponding to the vanishing eigenvalue. In order to calculate this eigenfunction we have

to compute all expansion coefficients $\{\underline{c}_n\}_{n=0}^\infty$ from (3.5) with $\lambda=0$ (note that for real eigenvalues the expansion coefficients obey the relation $\underline{c}_n = \underline{c}_{-n}^*$), i.e.

$$\begin{aligned} W_{st}(x, \theta) &= \sum_{m=0}^{\infty} \underline{c}_0^m \psi_m(x) + \sum_{m=0}^{\infty} \sum_{n=1}^{\infty} 2(\text{Re } \underline{c}_n^m) \\ &\quad \cdot \cos(n\theta) \psi_m(x) - 2(\text{Im } \underline{c}_n^m) \sin(n\theta) \psi_m(x). \end{aligned} \quad (3.12)$$

The stationary distribution in x , i.e. the phase averaged asymptotic distribution (see (2.30)) is given in terms of the coefficients $\{\underline{c}_0^m\}$ by

$$\hat{W}_{st}(x) = \int_0^{2\pi} W_{st}(x, \theta) d\theta = 2\pi \sum_{m=0}^{\infty} \underline{c}_0^m \psi_m(x). \quad (3.13)$$

In a first step we have to determine the coefficient-vector \underline{c}_0 . Inserting (3.6) into (3.5) for $n=0$ and using $\underline{c}_1 = \underline{c}_{-1}^*$ we find the solvable linear algebraic equation for \underline{c}_0

$$[\mathbf{Q}_0(0) + 2 \text{Re}(\mathbf{S}_0(0) \mathbf{Q}^+)] \underline{c}_0 = 0, \quad (3.14)$$

where $\mathbf{S}_0(0)$ is given in terms of the infinite matrix continued fraction (3.8) for $\lambda=0$. The other coefficients may be determined from \underline{c}_0 and the matrices $\mathbf{S}_n(0)$, occurring in the downward iteration procedure (3.7) as intermediate results, by

$$\underline{c}_n = \mathbf{S}_{n-1} \mathbf{S}_{n-2} \dots \mathbf{S}_0 \underline{c}_0. \quad (3.15)$$

The normalization of $\hat{W}_{st}(x)$ and $W_{st}(x, \theta)$ is given by

$$N = \int_{-\infty}^{\infty} \hat{W}_{st}(x) dx = 2\pi \sum_{m=0}^{\infty} \underline{c}_0^{2m} r_m, \quad (3.16)$$

where r_n can be determined iteratively with

$$\begin{aligned} r_0 &= \sqrt{2/\alpha} \pi^{1/4} \\ r_{n+1} &= \sqrt{\frac{2n+1}{2n+2}} r_n. \end{aligned} \quad (3.17)$$

In Figs. 1 a–d the altitude charts of the stationary distribution are shown for $D=0.1$ and $\omega_0=1$ for increasing values of the modulation strength A . As shown in Sect. 2.2 the two-variable stationary distribution is identical to the asymptotic time dependent probability $P_{st}^\phi(x, t)$ of the one dimensional FPE (2.4) if θ is interpreted as a scaled time. For small modulation strength A (Fig. 1 a) the distribution is peaked near the potential minima $x = \pm 1$ in the whole period $\theta = 0 \dots 2\pi$ ($t = 0 \dots T$). Close to the line $x=0$ we find craters in the distribution, i.e. regions which are avoided by the system. The most probable path of

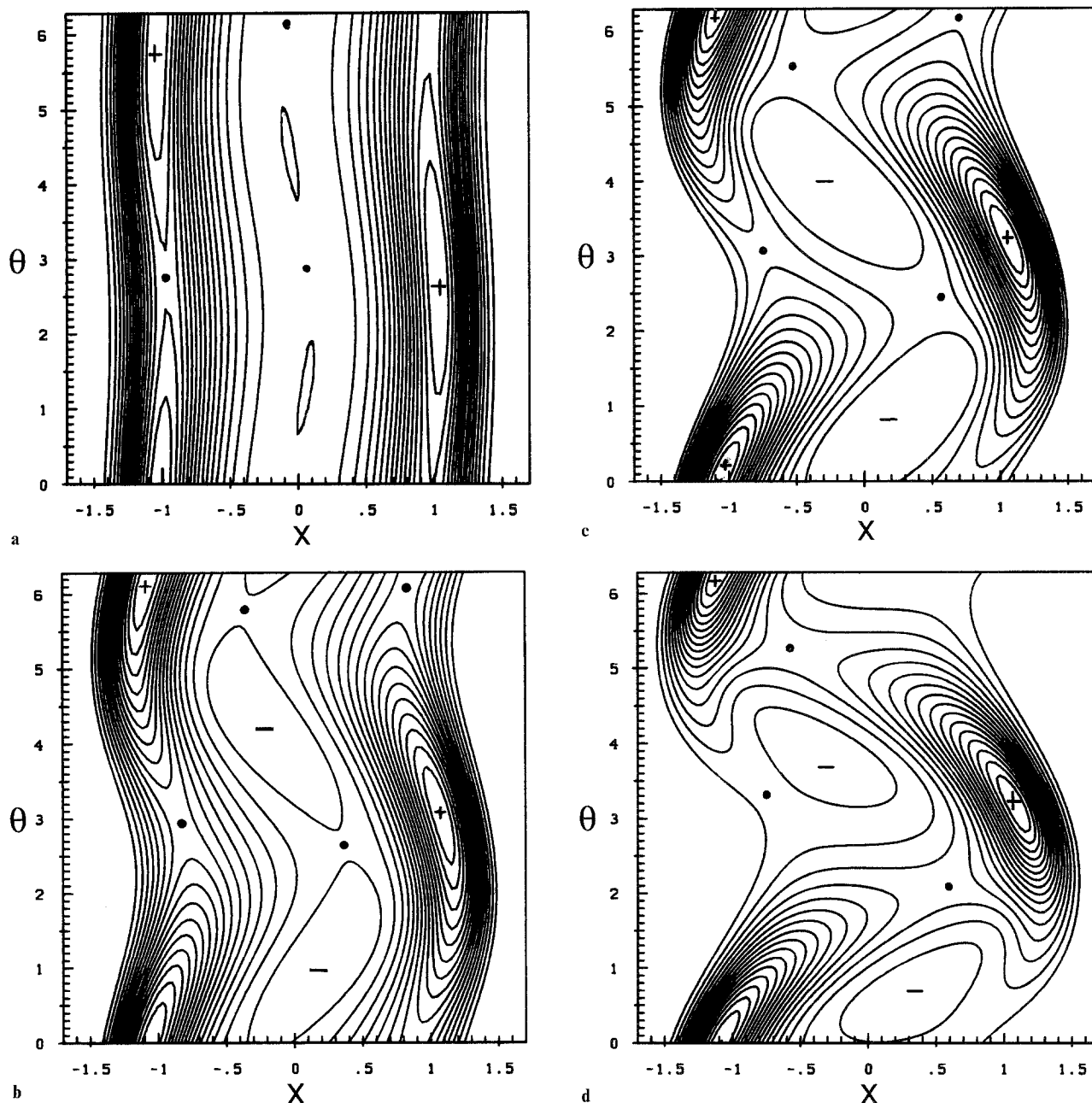


Fig. 1a-d. The altitude charts of the stationary probability (3.15) of the two dimensional FPE (2.10) is plotted at $\omega_0=1$ and $D=0.1$ for $A=0.1$ (a), $A=0.5$ (b), $A=0.75$ (c) and $A=1$ (d). The lines are equidistant in each figure; + denotes a maximum and - denotes a minimum and a full circle denotes the position of a saddle point

the system dynamics is along the line $x \sim \pm 1$, i.e. the system remains within one region of attraction. Note, however, that even in this case the system has to cross one of the saddle points (This kind of saddle points are denoted in the following by S_0). For increasing modulation strength A (Fig. 1 b) the lines of constant probability become more and more distorted towards the line $x=0$. For further increasing A (Fig. 1 c) the saddle points between the regions of attraction (this kind of saddle points are denoted in the following

by S_1) attain approximately the same probabilistic weight as the saddle points S_0 ; the escape process is now strongly enhanced by the modulation. For larger A -values (Fig. 1 d) it is more probable to escape from one region of attraction as compared to the sojourn in one well during one period. For further increasing modulation strength A , the topology of $W_{st}(x, \theta)$ changes. The saddle points S_0 vanish at some value of A . When the saddle points S_0 have vanished it is very improbable for the system to stay in the

region of attraction within one period; thus, the system follows the external modulation with a certain phase shift.

Adiabatic probability distribution. For extremely small frequencies of the external field we can neglect the derivative of θ with respect to time in (2.9), i.e. $\theta = \text{const}$. The stochastic differential equation for x

$$\dot{x} = x - x^3 + A \sin(\theta) + \xi(t) \quad (3.18)$$

contains the parameter θ . The stationary probability of (2.10) is given by

$$W_{ad}(x, \theta) = Z^{-1} \exp \left\{ -\frac{1}{D} \left[-\frac{1}{2} x^2 + \frac{1}{4} x^4 - A x \sin(\theta) \right] \right\}, \quad (3.19a)$$

The function $W_{ad}(x, \theta)$ with constant Z , however, cannot be interpreted as the asymptotic (large time) one dimensional probability in x , where θ plays the role of a scaled time, since the integral over x is not independent of θ , i.e. the normalization is not conserved. The normalization Z is thus not a constant, but rather depends on θ . Factorizing Z into a θ -dependent and an θ -independent part, we find

$$W_{ad}(x, \theta) = \frac{1}{Z_0} \exp(-x^4/(4D) + x^2/(2D) + A x/D \sin(\theta)) \cdot \left(\sum_{n=0}^{\infty} \frac{1}{n!} \left(\frac{A^2 \sin^2 \theta \sqrt{2D}}{4D^2} \right)^n \mathcal{D}_{-n-1/2}(-1/\sqrt{2D}) \right)^{-1} \quad (3.19b)$$

where

$$Z_0 = \exp(1/(8D)) (2D)^{1/4} \sqrt{\pi} \quad (3.19c)$$

and $\mathcal{D}_n(x)$ denote parabolic cylinder functions.

In our system there are three typical time scales, the modulation period $T_M = 2\pi/\omega_0$, the escape time $T_E = 1/\lambda_0 \approx \exp(\Delta V/D)$ and the period of the well oscillator $T_w = \pi$. The adiabatic approach is valid if T_M is much larger than the escape time T_E , i.e. $\omega_0 \ll \exp(-\Delta V/D)$. Thus for decreasing D the adiabatic approach (3.19) becomes worse. In Fig. 2, the adiabatic stationary probability (3.19) is plotted for $D=0.1$ and $A=0.1$. Although the qualitative agreement with the numerical result for $\omega_0=1$ (Fig. 1a) is quite good we notice that the sensitivity of the system against the periodic modulation is typically larger in the limit of vanishing driving frequency ω_0 .

Phase averaged probability distribution. The phase averaged stationary distribution (2.30) $\hat{W}_{st}(x)$ has

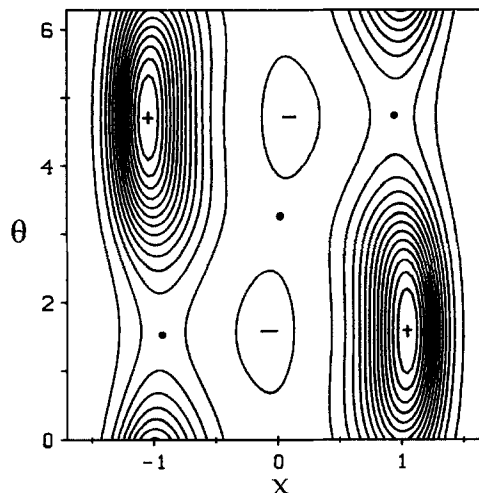


Fig. 2. The altitude charts of the adiabatic stationary probability (3.19 b) for $D=0.1$ and $A=0.1$

some interesting behavior with varying modulation frequency. In Fig. 3a the numerically evaluated stationary probability $\hat{W}_{st}(x)$ is plotted for various values of the modulation strength A at a modulation frequency $\omega_0 = 10 \gg \lambda_0$ (Kramers rate (2.31)). For increasing A the distribution smears out and the maxima are shifted toward the saddle point $x=0$. This implies correctly (as shown in the next section) an increasing transition rate for increasing A . For large modulation strength, the maxima of the distribution tend both to zero and the distribution becomes unimodal. This behavior again shows that for large A , the distribution is following the external modulation. The system does not feel much of the bistability of the potential.

For an extremely small modulation frequency $\omega_0 = 0.001 \ll \lambda_0$, however, the effect of the modulation is to sharpen $\hat{W}_{st}(x)$ and to shift the maxima to larger values. Figure 3b shows $\hat{W}_{st}(x)$ for $\omega_0 = 0.001$ and some values of A . This behavior is in agreement with an adiabatic approach for the probability distribution presented in Sect. 4.2. In spite of the increase of the Arrhenius factor $\hat{W}_{st}(\text{saddle})/\hat{W}_{st}(\text{well})$ of the phase averaged stationary probability density, the activation rate increases with increasing modulation strength A . This feature is discussed further in Sect. 4.2.

3.3. Transition rates, smallest non-vanishing eigenvalue

With our MCF technique we can numerically determine all eigenvalues (real and complex) of the two dimensional FPE (2.10). Performing the numerical calculations described in Sect. 3.1, we find apart from the purely imaginary branch only real eigenvalues.

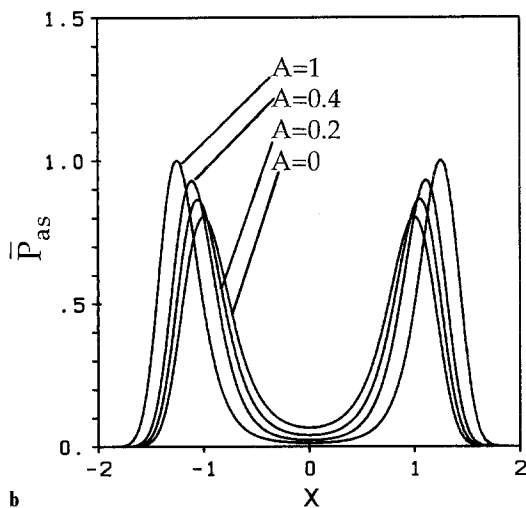
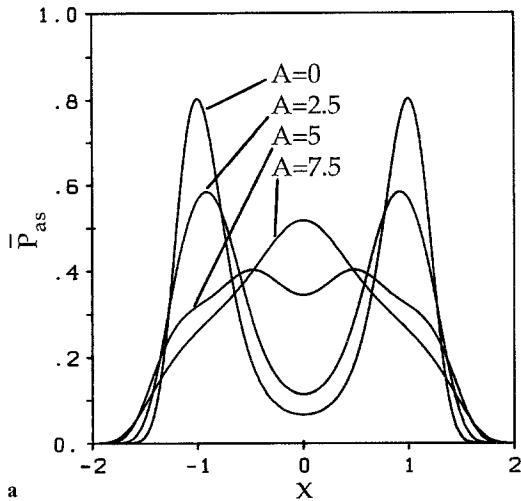


Fig. 3a and b. The stationary, phase averaged probability (3.16) is shown for a large frequency $\omega_0=10$ (a) and for a small frequency $\omega_0=0.001$ (b) for various values of the modulation strength A . In both figures the noise strength was $D=0.1$

Those real branches start for $A=0$ at the eigenvalues of \mathbf{L}_0 and remain real for increasing A . We did not find any bifurcations of two real eigenvalues into a complex-valued eigenvalue, neither for small nor for large modulation frequencies. Thus, the smallest non-vanishing real eigenvalue represents the escape rate, we are interested in (see also Sect. 2.3 for remarks on the small frequency limit). Figure 4 (solid lines) depict the rate enhancement

$$\mu(A, \omega_0) = \frac{\lambda_{\min}(A, \omega_0)}{\lambda_0} - 1, \quad (3.20)$$

as a function of the modulation strength A for the modulation frequency, $\omega_0=10$ and the noise strength $D=0.1$. Here λ_{\min} denotes the smallest non-vanishing real eigenvalue (2-escape rate). The rate enhancement increases with increasing modulation strength ($\propto A^2$

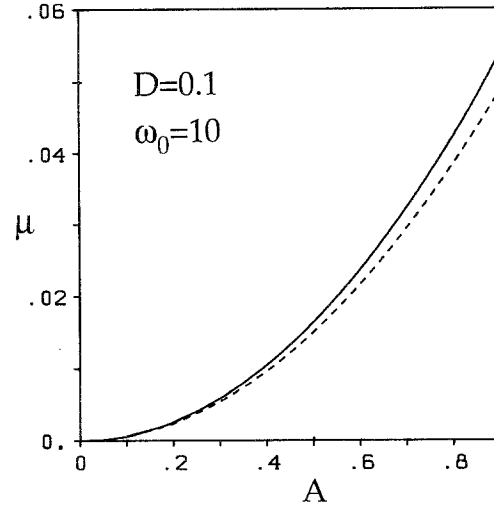


Fig. 4. The transition rate enhancement μ (for a definition see (3.20)) obtained numerically (full lines) is compared with the result due to the averaging theory (dashed lines) (4.9) for $\omega_0=10$

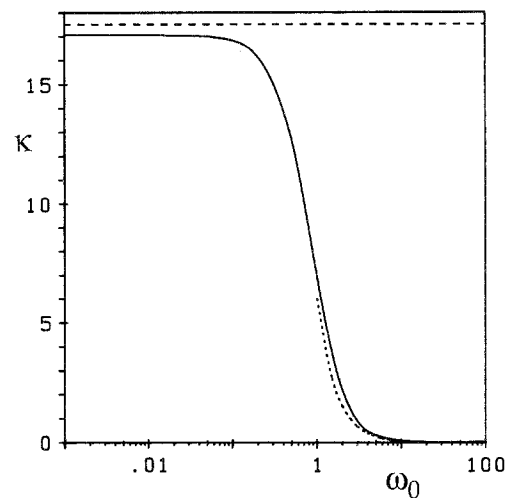


Fig. 5. The rate enhancement factor κ (for a definition see (4.9)) is plotted as a function of the modulation frequency ω_0 at $D=0.1$. The numerical curve (full line) connects the high frequency results due to the averaging theory (4.9) (dotted line) with the adiabatic approach (4.20) (dashed line)

for small A). In Fig. 5 the rate-enhancement factor $\kappa \equiv \mu/A^2$ is plotted as a function of the modulation frequency. For large frequencies the enhancement factor vanishes $\propto 1/\omega_0^2$. For decreasing frequencies, κ increases up to a finite value, which is reached approximately at $\omega_0 \approx 2\pi\lambda_0$ (Kramers rate of the unperturbed system). For further decreasing modulation frequency the rate remains constant (plateau). In Fig. 5 we have also plotted the approximative results due to an averaging theory valid for large modulation frequencies (dotted line) and that of an approximate adiabatic rate theory for small frequencies (dashed

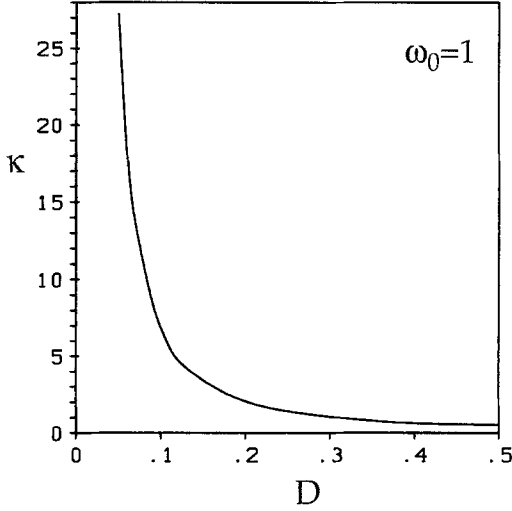


Fig. 6. The rate enhancement factor κ (for a definition see (4.9)) obtained numerically is shown as a function of the noise strength D for $\omega_0=1$

line). Both approximations are discussed in Sect. 4. In Fig. 6 the rate enhancement is plotted as a function of the noise strength D . The curve exhibits a monotonic increase for decreasing noise strength.

4. Theories for the activation rates and probability distributions

In this section theoretical approximations for the modulation enhancement are presented and compared with the numerical results.

4.1. Averaging theory for moderate to large frequencies

Here we assume, that the modulation frequency is larger than all typical frequencies of the system. In the limit of infinite large frequencies the modulation effects vanish in overdamped systems, since the system does not allow for a infinite fast reaction. In other words, the linear response tends to zero $\propto A/\omega_0^2$. This fact allows the following averaging procedure which is similar to the Bogoliubov-averaging technique (see for instance in [3a]) for underdamped nonlinear oscillators. In a first step we start from the Langevin equation (2.3) which can be written in the form

$$\frac{d}{dt} \left[x + \frac{A}{\omega_0} \cos(\omega_0 t + \phi) \right] = h(x) + \xi(t)$$

$$h(x) = x - x^3. \quad (4.1)$$

Introducing the variable $z = x + (A/\omega_0) \cos(\omega_0 t + \phi)$, (4.1) reads

$$\dot{z} = h \left(z - \frac{A}{\omega_0} \cos(\omega_0 t + \phi) \right) + \xi(t). \quad (4.2)$$

For large frequencies ω_0 the dynamics of the variable z is controlled by the noise ξ and is thus only a weak function of $\omega_0 t + \phi$. The next step consists in averaging over the random phase ϕ (which for uniformly distributed ϕ is equivalent with a time averaging over the period $T = 2\pi/\omega_0$) by assuming z to be nearly constant within one period of oscillation. Thus, in a first approximation z takes on a fixed average value \bar{z} , i.e.

$$\langle f(z) g(\cos(\omega_0 t + \phi)) \rangle \approx f(\bar{z}) \langle g(\cos(\omega_0 t + \phi)) \rangle, \quad (4.3)$$

and the averaged Langevin equation (4.2) has the form

$$\dot{\bar{z}} = \left\langle h \left(z - \frac{A}{\omega_0} \cos(\omega_0 t + \phi) \right) \right\rangle + \xi(t). \quad (4.4)$$

Performing the average over the random phase ϕ in (4.4) yields in virtue of

$$\begin{aligned} \langle \cos^2(\omega_0 t + \phi) \rangle &= \frac{1}{2} \\ \langle \cos^3(\omega_0 t + \phi) \rangle &= 0 \end{aligned} \quad (4.5)$$

the effective Langevin equation in \bar{z} , i.e.

$$\dot{\bar{z}} = \bar{z} \left(1 - \frac{3A^2}{2\omega_0^2} \right) - \bar{z}^3 + \xi(t). \quad (4.6)$$

The Langevin equation (2.3) is thus approximated by an effective Langevin equation, describing the overdamped stochastic motion in the averaged bistable potential

$$V_{av}(\bar{z}) = \frac{1}{4} \bar{z}^4 - \frac{1}{2} \left(1 - \frac{3A^2}{2\omega_0^2} \right) \bar{z}^2. \quad (4.7)$$

Here the modulation parameters A , ω_0 enter solely in the combination A/ω_0 . An approach for the escape rate r is obtained by using the Kramers formula [1] valid for *small noise strength* D , i.e.

$$\begin{aligned} r(A, \omega_0) &= \lambda(A, \omega_0)/2 \\ &= \frac{1}{\pi} \sqrt{|V_{av}''(0)| V_{av}''(z_{\min})} \exp \left\{ -\frac{AV_{av}}{D} \right\} \end{aligned} \quad (4.8)$$

for the effective potential (4.7). Here z_{\min} denotes the position of one of the potential minima. To be consistent with the averaging procedure we have to assume

small values for A/ω_0 . In leading order we finally obtain for the rate enhancement

$$\mu = \frac{\lambda(A, \omega_0)}{\lambda_0} - 1 = \frac{3}{4} \left(\frac{A}{\omega_0} \right)^2 \left(\frac{1}{D} - 2 \right) = \kappa_{\text{Th}} A^2, \quad (4.9)$$

where κ_{Th} is independent of A . The enhancement μ increases with decreasing frequency and increases with increasing modulation strength. This behavior is in agreement with the numerical results of Sect. 3.3. In Fig. 4, (4.9) (dotted line) is compared with the numerical results for $\omega_0 = 10$. As expected from the theory, we find good agreement for not too large values of A/ω_0 . The agreement becomes still better for increasing frequency as seen in the table below, where we compare the numerical κ values with the theoretical values (4.9) (see also Fig. 5).

ω_0	1	10	50
κ_{num}	7.016	0.065	0.0025
κ_{Th}	6.0	0.060	0.0024

The A^2 -law in (4.9) is confirmed very well by the numerical investigations. The numerically calculated quantity κ_{num} has turned out to be constant to a high degree of accuracy for small values of A/ω_0 .

The averaging theory above also provides probability distributions for the averaged variable \bar{z} . The stationary distribution of \bar{z} corresponding to (4.6) reads

$$W_{\text{av}}(\bar{z}) = Z^{-1} \exp \left\{ -\frac{V_{\text{av}}(\bar{z})}{D} \right\}, \quad (4.10)$$

with

$$Z = \sqrt{\pi} (2D)^{+1/4} \exp \left(\frac{(1 - 3A^2/(2\omega_0^2))^2}{8D} \right) \cdot \mathcal{D}_{-1/2} \left(-\frac{1 - 3A^2/(2\omega_0^2)}{\sqrt{2D}} \right), \quad (4.11)$$

and $\mathcal{D}_\nu(x)$ being a parabolic cylinder function. The maxima of the averaged distribution are shifted to smaller values for increasing modulation strengths A , i.e.

$$\bar{z}_{1,2}^s = \pm \left| 1 - \frac{3A^2}{4\omega_0^2} \right|, \quad (4.12)$$

and the barrier height is reduced to

$$\Delta V_{\text{av}}(A, \omega_0) = \frac{1}{4} - \frac{3}{4} \frac{A^2}{\omega_0^2}. \quad (4.13)$$

Shifts of the maxima, the reduction of the potential height, as well as the bimodal-monomodal transition are also obtained numerically for the phase averaged distribution $\bar{P}_{\text{as}}(x)$ in Sect. 3.2. The agreement with the formulas above, however, is only qualitatively; the quantitative agreement is rather poor. This is not surprising, since the distribution of an averaged variable \bar{z} need not necessarily agree with the averaged distribution of the variable z . The transition rate, however, is approximated very well with the very same effective Langevin approach (4.6). On the other hand, if we compare the Kramers rate obtained from another hypothetical effective Langevin equation, where the underlying potential is derived from the *exact phase averaged distribution*, i.e. $V_{\text{as}}(x) = -D \ln \bar{P}_{\text{as}}(x)$, the agreement with the numerically evaluated escape rate is rather poor. Thereupon we can draw the following conclusion: *The escape rate obtained from an effective Langevin equation, where the underlying potential is obtained from the exact phase averaged distribution $\bar{P}_{\text{as}}(x)$ is not correct. The two-dimensional escape process is better approximated by the dynamics of the averaged variable \bar{z} .*

Moreover, from (4.12) one obtains a critical value for A , when the bimodal distribution $W_{\text{av}}(\bar{z})$ becomes monomodal

$$A_c = \omega_0 \sqrt[4]{\frac{4}{3}}. \quad (4.14)$$

For increasing frequencies the critical value of A also increases. This behavior is due to the decreasing sensitivity of the system for increasing modulation frequencies. The precise value of A_c in (4.14) can not be compared to that obtained numerically for the phase averaged probability distribution, since: (i) both distributions (phase averaged distribution and distribution of the averaged variable) do not agree for the reasons explained above and (ii) the ratio $A_c/\omega_0 = \sqrt[4]{4/3}$ is not small. Thus we are outside the region of support of the averaging theory. In contrast, the adiabatic potential

$$V_{\text{ad}}(x, \theta) = \frac{1}{4} x^4 - \frac{1}{2} x^2 - Ax \sin \theta + D \ln f(\theta) \quad (4.15)$$

where

$$f(\theta) = \sum_{n=0}^{\infty} \frac{1}{n!} \left(\frac{A^2 \sin^2 \theta \sqrt{2D}}{4D^2} \right)^n \mathcal{D}_{-n-1/2}(-1/\sqrt{2D}) \quad (4.16)$$

is only bimodal (during the whole period 2π) for $A < A_0 = \sqrt[4]{4/27}$ [17], formally for all ω_0 .

4.2. Adiabatic rate theory for very small frequencies

For small frequencies our averaging technique in Sect. 4.1 is not valid. In the case of extremely small frequencies, i.e. $\omega_0 \ll \text{escape rate}$, we can construct an adiabatic rate theory. The adiabatic potential corresponding to the two dimensional stationary adiabatic probability distribution is given by (4.15). A different initial phase ϕ of the field corresponds to a different value of θ . The idea consists in calculating the escape rate out of one potential well for fixed θ and then to average over the uniformly distributed phase θ . The extrema of the adiabatic potential are given by

$$\begin{aligned} x_u &= -A \sin \theta + O(A^3) \\ x_s &= 1 + \frac{A}{2} \sin \theta - \frac{3}{8} A^2 \sin^2 \theta + O(A^3), \end{aligned} \quad (4.17)$$

where x_u is the position of the saddle point and x_s is the position of a minimum of the potential. The barrier height is given for small A by

$$\Delta V_{\text{ad}}(\theta) = \frac{1}{4} + A \sin \theta + \frac{3}{4} A^2 \sin^2 \theta. \quad (4.18)$$

Note, that $\langle \Delta V(\theta) \rangle_\theta = 1/4 + 3A^2/8 > \Delta V(A=0) = 1/4$ is on the average larger than the barrier height with $A=0$. The θ -dependent Kramers rate is thus given by (see (4.8))

$$\begin{aligned} r(A, \theta) &= \frac{1}{\sqrt{2\pi}} \left(1 + \frac{3}{4} A \sin \theta - \frac{69}{32} A^2 \sin^2 \theta \right) \\ &\cdot \exp \left\{ - \left(\frac{1}{4D} + \frac{A}{D} \sin \theta + \frac{3}{4D} A^2 \sin^2 \theta \right) \right\}. \end{aligned} \quad (4.19)$$

Here, terms in the prefactor of order higher than A^2 are neglected. For small modulation strength $A/D \rightarrow 0$ and $D \rightarrow 0$ (steepest decent approach) we can expand the exponent in (4.19). Averaging over θ yields for the rate enhancement (3.23), (see also Ref. 10)

$$\mu(A, \omega=0) = \frac{\langle r(A, \theta) \rangle}{r(A=0)} - 1 = \left(\frac{1}{4D^2} - \frac{3}{4D} \right) A^2 = \kappa_{\text{ad}} A^2. \quad (4.20)$$

Since corrections terms to the steepest decent approximation, used to derive the Kramers formula, contribute to the terms of order D^0 (which occur after averaging (4.19)) we have canceled this term in order to keep consistently only the *leading order contributions* for small noise strength D . We again find a rate enhancement, being proportional to A^2 . At first glance this seems to be surprising, since the θ -dependent potential height $\Delta V(\theta)$ is on the average larger than the

barrier in the absence of modulation. The average over the exponential function of $\Delta V_{\text{ad}}(\theta)$ weights smaller potential heights (for some values of θ) exponentially higher than large barrier heights, leading to the rate enhancement. The prefactor κ_{ad} is typically larger than κ_{Th} in the large-frequency regime. In Fig. 5 κ_{ad} is compared against the numerical results. The exact value for κ approaches κ_{ad} in (4.20) for vanishing frequencies (up to steepest descent errors) satisfactorily. Note, however, that the rate enhancement approaches the adiabatic limit (4.20) only for very small modulation frequencies $\omega_0 \lesssim 2\pi \cdot (\text{escape rate})$. For a modulation frequency which is comparable to the typical intra-well frequency ($\omega_0=2$) the rate enhancement is *well below* its adiabatic value. Thus a rate theory [19] based on a two state master type equation approach with the transition rate taken from the adiabatic approach is questionable for modulation frequencies larger than the thermal hopping frequency.

For the phase averaged probability distribution we can also find an adiabatic expression. The adiabatic stationary probability distribution is given by (3.19). Performing the θ -average, i.e.

$$\bar{P}_{\text{ad}}(x) = \frac{1}{2\pi} \int_0^{2\pi} W_{\text{ad}}(x, \theta) d\theta \quad (4.21)$$

we find in leading order in A

$$\bar{P}_{\text{ad}}(x) = \frac{1}{Z} \exp \left(- \frac{V(x)}{D} \right) \cdot \left(1 + \frac{1}{4} \frac{A^2}{D^2} x^2 \right) \quad (4.22)$$

In order to derive (4.22) we have expanded the sum in the denominator in (3.19b) up to the order A^2 . To perform the θ -integration we have used the expansion of $\exp(z \sin \theta)$ and $\exp(z \cos \theta)$ in terms of modified Bessel functions $I_n(x)$. A consistent truncation of the resulting infinite series then yields (4.22). The averaged stationary probability $\bar{P}_{\text{ad}}(x)$ shows maxima at

$$x_{1,2}^2 = 1 + \frac{A^2}{2D} + O(A^4) \quad (4.23)$$

and a minimum at $x_0=0$. The barrier height of $U_{\text{ad}}(x) \equiv -D \ln \bar{P}_{\text{ad}}(x)$ is increased due to the modulation, i.e.

$$\Delta U_{\text{ad}} = \frac{1}{4} + \frac{A^2}{2D} + O(A^4). \quad (4.23)$$

The shift of the extrema and the increased barrier height are in qualitative agreement with the numerical results for the phase averaged distribution in Sect. 3.2.

Although the barrier heights of the adiabatic potential $U_{\text{ad}}(x)$ increase for increasing modulation strength, the activation rates also increase. Calculating the Kramers rate within the effective potential $U_{\text{ad}}(x)$, we find a rate-depression $\mu = 1 - A^2/(4D^2)(1 - 2D)$. Just as in the high frequency case in Sect. 4.1 we conclude, that the potential of the exact phase averaged distribution does not produce the correct transition rates.

5. Comment on external fields with finite coherence times

In Sect. 2.1 we pointed out, that the coherently (perfect periodic) modulated stochastic system are non mixing. The origin for this non-mixing property is the one dimensional dispersion free dynamics (2.18) of the x -integrated probability density (2.20). A realistic model, however, has to take into account a finite coherence time for the modulation mechanism, since no experimental setup produces a real single-frequency signal. In the case of a laser modulation for instance, the coherence times are well known and measurable. In order to include a coherence destroying mechanism in our model, we add a fluctuating part to the frequency ω_0 , modeled by a Gaussian white noise. The extended Langevin equations read

$$\begin{aligned}\dot{x} &= x - x^3 + A \sin \theta + \xi(t) \\ \dot{\theta} &= \omega_0 + \xi_f(t),\end{aligned}\quad (5.1)$$

with

$$\begin{aligned}\langle \xi(t) \rangle &= \langle \xi_f(t) \rangle = 0 \\ \langle \xi(t) \xi(t') \rangle &= 2D \delta(t-t'), \quad \langle \xi_f(t) \xi_f(t') \rangle = 2Q \delta(t-t') \\ \xi(t), \xi_f(t) &: \text{Gaussian.}\end{aligned}\quad (5.2)$$

The term

$$F(t) \equiv A \sin \theta = A \sin(\omega_0 t + \phi + \int \xi_f(t') dt') \quad (5.3)$$

may be interpreted as a non-Gaussian colored noise with zero mean (due to ϕ -averaging) with the correlation function [6]

$$\langle F(t) F(t') \rangle = A^2 \exp(-Q|t-t'|) \cos(\omega_0(t-t')). \quad (5.4)$$

From (5.4) we recognize that the frequency-noise strength Q has the physical meaning of an inverse

coherence time τ_ω i.e. $\tau_\omega = 1/Q$. The Fokker-Planck equation corresponding to (5.1) and (5.2) reads

$$\begin{aligned}\frac{\partial W(x, \theta, t)}{\partial t} &= \left(\mathcal{L}_0 - \frac{\partial}{\partial x} A \sin \theta - \omega_0 \frac{\partial}{\partial \theta} \right. \\ &\quad \left. + \frac{1}{\tau_c} \frac{\partial^2}{\partial \theta^2} \right) W(x, \theta, t) \\ &\equiv \mathcal{L}_2^+ W(x, \theta, t).\end{aligned}\quad (5.5)$$

The adjoint Fokker-Planck operator

$$\mathcal{L}_2^+ = \mathcal{L}_0^+ + \frac{\partial}{\partial x} A \sin \theta + \omega_0 \frac{\partial}{\partial \theta} + \frac{1}{\tau_c} \frac{\partial^2}{\partial \theta^2} \quad (5.6)$$

has the x independent eigenfunctions $\varphi_{0n}(\theta)$, obeying

$$\omega_0 \varphi'_{0n}(\theta) + \frac{1}{\tau_c} \varphi''_{0n}(\theta) = -\lambda_{0n} \varphi_{0n}(\theta) \quad (5.7)$$

Using periodic boundary conditions, i.e. $\varphi_{0n}(\theta) = \varphi_{0n}(\theta + 2\pi)$, one finds

$$\begin{aligned}\varphi_{0n}(\theta) &= \exp(-in\theta) \\ \lambda_{0n} &= in\omega_0 + \frac{1}{\tau_c} n^2\end{aligned}\quad (5.8)$$

The additional phase diffusion term makes the former purely imaginary branch of eigenvalues complex with a finite real part. The Fokker-Planck equation (5.5) is therefore strongly mixing [15]. The probability distributions $P(x, t)$ and $W(x, \theta, t)$ approach a steady state for any initial distribution. The correlation function $\langle x(t) x(t') \rangle$ which exhibits undamped oscillations [12] for infinite coherence times ($\tau_c \rightarrow \infty$) leading to δ -spikes in the power spectrum, are now regularized for τ_c finite. Thus the power spectrum shows Lorentzians with finite peak heights and widths [12]. In a future publications the influence of finite coherence times on the ‘‘stochastic resonance’’ will be discussed in detail.

6. Conclusions

We have considered the activation process in a bistable potential with thermal noise being driven by an external periodic field. The dynamics of the nonstationary Markovian process has been described in terms of quasi spectral properties, where the quasi-eigenvalues have been proven to coincide with the eigenvalues of an extended two-dimensional time homogeneous FPE. The activation process has been discussed explicitly in terms of the asymptotic periodic probability densities and the transition rates. Both quantities have been obtained numerically using a

matrix continued fraction method. Moreover, approximate theories for small and large modulation frequencies have been presented. The results of these approximations have been compared with the numerical data. At this point I want to emphasize, that the numerical errors in all numerical evaluated curves are within the line thickness.

The technique presented in this paper is not restricted to the quartic double well potential (2.1), but holds for very general potentials $V(x)$, such as a periodic potential or a asymmetric potential. It opens a huge field of applications in quantum optics (periodic modulated lasers), surface science (classical model for laser assisted desorption processes), transport theory (field induced mobility and conductivity effects) and in the theory of superconducting devices (Josephson junctions with microwave radiation [10]).

I want to thank Prof. Dr. P. Hänggi and Dr. F. Marchesoni (University Perugia/Italy) for many fruitful discussions on problems related to the paper. Further I should like to thank Prof. R. Fox and Prof. R. Roy for drawing my attention to the problem of "stochastic resonance" during a visit at the Georgia Institute of Technology, Atlanta/USA. Moreover I want to thank Prof. Fulinski and his group (especially Dr. A. Kleczkowski) at the Jagiellonian University in Krakow/Poland for hospitality and many discussions on this topic.

Appendix A: Explicit expressions for the matrices \mathbf{L}_0 and \mathbf{B}

The matrices \mathbf{L}_0 and \mathbf{B} are of course dependent on the special choice of the shape function $\rho_0(x)$. For $\rho_0(x)=1$ we find

$$\begin{aligned} L_0^{n,m} = & \left\{ -\frac{1}{2} + \frac{3}{2\alpha^{2n}} + \frac{3}{4\alpha^2} - \frac{1}{2} D\alpha^2(2n+1) \right\} \delta_{n,m} \\ & + \left\{ \frac{1}{2} + \frac{1}{\alpha^2} - \frac{n}{2\alpha^2} + \frac{D}{2}\alpha^2 \right\} \sqrt{n(n-1)} \delta_{n,m+2} \\ & + \left\{ -\frac{1}{2} + \frac{3}{2d^2} + \frac{n}{2\alpha^2} + \frac{D}{2}\alpha^2 \right\} \\ & \cdot \sqrt{(n+1)(n+2)} \delta_{n,m-2} \\ & - \frac{1}{4\alpha^2} \sqrt{n(n-1)(n-2)(n-3)} \delta_{n,m+4} \\ & + \frac{1}{4\alpha^2} \sqrt{(n+1)(n+2)(n+3)(n+4)} \delta_{n,m-4} \\ B^{n,m} = & -\frac{\alpha}{\sqrt{2}} (\sqrt{n+1} \delta_{n,m-1} - \sqrt{n} \delta_{n,m+1}) \end{aligned} \quad (\text{A.1})$$

The shape function $\rho_0(x)=1$ has turned out to be convenient for the calculation of the stationary distribution. For the eigenvalues it has turned out, that

the shape function $\rho_0(x)=\psi_0(x)$, where $\psi_0(x)$ is given in (3.1) produces a better convergence. In this case the matrices \mathbf{L}_0 and \mathbf{B} take the simpler form

$$\begin{aligned} L_0^{n,m} = & n \left(1 - \frac{3}{2\alpha^2} n \right) \delta_{n,m} + \left(1 - \frac{3}{2\alpha^2} (n-1) + 2\alpha^2 D \right) \\ & \cdot \sqrt{n(n-1)} \delta_{n,m+2} - \frac{n}{2\alpha^2} \sqrt{(n+1)(n+2)} \delta_{n,m-2} \\ & - \frac{1}{2\alpha^2} \sqrt{n(n-1)(n-2)(n-3)} \delta_{n,m+4} \\ B^{n,m} = & -a\sqrt{2n} \delta_{n,m+1} \end{aligned} \quad (\text{A.2})$$

Appendix B: Master equation approach for the time dependent phase averaged reduced probability

In a first step we perform the Laplace transform of (2.13). With (s real)

$$\tilde{c}_n = \int_0^\infty \exp(-st) c_n(x, t) dt, \quad (\text{B.1})$$

we obtain

$$\begin{aligned} -c_n(x, 0) = & (\mathcal{L}_0 - (in\omega_0 + s) 1) \tilde{c}_n - \frac{1}{2} iA \mathcal{L}_1 \tilde{c}_{n+1} \\ & + \frac{1}{2} iA \mathcal{L}_1 \tilde{c}_{n-1}, \end{aligned} \quad (\text{B.2})$$

with

$$\mathcal{L}_1 = \frac{\partial}{\partial x}. \quad (\text{B.3})$$

The function $c_n(x, 0)$ can be determined from the initial distribution. If we assume a factorized initial probability with a uniform θ dependence, i.e.

$$W(x, \theta, t=0) = W_0(x) \quad (\text{B.4})$$

we find for $c_n(x, 0)$

$$\begin{aligned} c_n(x, 0) = & \frac{1}{2\pi} \int_0^{2\pi} W(x, \theta, t=0) \exp(-in\theta) d\theta \\ = & \delta_{n,0} W_0(x). \end{aligned} \quad (\text{B.5})$$

Thus, the system of partial differential equations (B.2) is homogeneous for $n \neq 0$. The transfer operators $\tilde{\mathbf{S}}_n$, defined by

$$\tilde{\mathbf{S}}_n(s) \tilde{c}_n(x, s) = \tilde{c}_{n+1}(x, s), \quad (\text{B.6})$$

obey the operator recursion

$$\begin{aligned} \tilde{\mathbf{S}}_{n-1}(s) = & -\frac{1}{2} iA [\mathcal{L}_0 - (in\omega_0 + s) 1 \\ & - \frac{1}{2} iA \mathcal{L}_1 \tilde{\mathbf{S}}_n(s)]^{-1} \mathcal{L}_1. \end{aligned} \quad (\text{B.7})$$

Since the functions $\tilde{c}_n(x, s)$ obey the relation

$$\tilde{c}_{-n}(x, s) = \tilde{c}_n^*(x, s), \quad (\text{B.8})$$

which follows from the fact, that $W(x, \theta, t)$ has to be real, we obtain from (B.2) for $n=0$

$$-W_0(x) = (\mathcal{L}_0 - s) \tilde{c}_0(x, s) + \mathcal{L}_1 \tilde{\mathbf{K}}(s) \tilde{c}_0(x, s) \quad (\text{B.9})$$

with the operator

$$\tilde{\mathbf{K}}(s) = -\text{Re}(iA S_0(s)). \quad (\text{B.10})$$

Using the convolution theorem for Laplace transforms we find the exact integro-differential equation for $c_0(x, t)$

$$\dot{c}_0(x, t) = \mathcal{L}_0 c_0(x, t) + \mathcal{L}_1 \int_0^t \mathbf{K}(t-t') c_0(x, t') dt' \quad (\text{B.11})$$

where the Laplace transform of the operator-kernel $\mathbf{K}(t-t')$ can be formally written as an infinite operator continued fraction

$$\tilde{\mathbf{K}}(s) = \text{Re} \left\{ \frac{A^2/4}{\mathcal{L}_0 - i\omega_0 - s - \mathcal{L}_1 \frac{A^2/4}{\mathcal{L}_0 - 2i\omega_0 - s - \dots \mathcal{L}_1}} \right\}. \quad (\text{B.12})$$

Since $c_0(x, t)$ is identical with the phase averaged one dimensional probability, i.e.

$$\bar{P}(x, t) = \frac{1}{2\pi} \int_0^{2\pi} W(x, \theta, t) d\theta = c_0(x, t). \quad (\text{B.13})$$

Equation (B.11) is an equation for the phase averaged probability distribution. The operator continued fraction (B.12) can be expanded in powers of A^2 , yielding in lowest order the integro-differential equation for $c_0(x, t)$

$$\dot{c}_0(x, t) = \mathcal{L}_0 c_0(x, t) - \frac{1}{4} A^2 \mathcal{L}_1 \int_0^t \exp(\mathcal{L}_0(t-t')) \cdot \cos(\omega_0(t-t')) \mathcal{L}_1 c_0(x, t') dt'. \quad (\text{B.14})$$

References

1. Kramers, H.A.: *Physica* **7**, 284 (1940)
2. For a overview, see: Hänggi, P.: *J. Stat. Phys.* **42**, 105 (1986)
3. (a) Hänggi, P., Riseborough, P.: *Am. J. Phys.* **51**, 347 (1983);
(b) Ryter, D., Talkner, P., Hänggi, P.: *Phys. Lett.* **93A**, 447 (1983)
4. (a) Arecchi, F.T., Califano, A.: *Phys. Lett.* **101A**, 443 (1984);
(b) Beasley, M.R., D'Humieres, D., Hubermann, B.A.: *Phys. Rev. Lett.* **50**, 1328 (1983)
5. Crutchfield, J.P., Hubermann, B.A.: *Phys. Lett.* **77A**, 407 (1980)
6. Carmeli, B., Nitzan, A.: *Phys. Rev. A* **32**, 2435 (1985)
7. (a) Munakata, T., Kawakatsu, T.: *Progr. Theor. Phys.* **74**, 262 (1985);
(b) Munakata, T.: *Progr. Theor. Phys.* **75**, 747 (1986)
8. Larkin, A.I., Ovchinnikov, Yu. N.: *J. Low Temp. Phys.* **36**, 317 (1986)
9. Chow, K.S., Ambegaokar, V.: *Phys. Rev. B* **38**, 11168 (1988)
10. (a) Devoret, H.M., Esteve, D., Martinis, J.M., Cleland, A., Clarke, J.: *Phys. Rev. B* **36**, 58 (1987);
(b) Devoret, M.H., Martinis, J.M., Esteve, D., Clark, J.: *Phys. Rev. Lett.* **53**, 1260 (1984)
11. (a) Mc Namara, B., Wiesenfeld, K., Roy, R.: *Phys. Rev. Lett.* **60**, 2626 (1988);
(b) Gammaitoni, L., Marchesoni, F., Menichella-Saetta, E., Santucci, S.: *Phys. Rev. Lett.* **62**, 349 (1989);
(c) R. Fox.: *Phys. Rev. A* **39**, 4/48 (1989)
12. Jung, P., Hänggi, P.: *Europhys. Lett.* **8**, 505 (1989)
13. Risken, H.: *The Fokker-Planck equation*. Springer Series in Synergetics, Vol. 18. Berlin, Heidelberg, New York: Springer 1984
14. Zeldovich, Yu.B.: (a) *Sov. Phys. JETP* **24**, 1006 (1967) [*Zh. Eksp. Teor. Fiz.* **51**, 1492 (1966)];
(b) *Sov. Phys. Usp.* **16**, 427 (1973) [*Usp. Fiz. Nauk.* **110** (1973) 139];
(c) V.I. Ritus, *Sov. Phys. JETP* **24**, 1041 (1967) [*Zh. Eksp. Teor. Fiz.* **51**, 1544 (1966)]
15. Hänggi, P., Thomas, H.: *Phys. Rep.* **88C**, 207 (1982)
16. For the case of a non-uniform distribution for the initial phases, see the footnotes in [12]
17. Debnath, G., Zhoo, T., Moss, F.: *Phys. Rev. A* **39**, 4323 (1989)
18. By a simple modification of the MCF expansion technique (see Chap. 9 of [13]) the eigenvalues $\lambda_{0n} = in\omega_0$ can also be found
19. Mc Namara, B., Wiesenfeld, K.: *Phys. Rev. A* **39**, 4854 (1989)

P. Jung
Institut für Mathematik
Universität Augsburg
Memminger Strasse 6
D-8900 Augsburg
Federal Republic of Germany